



Search for the pair production of scalar top quarks in acoplanar charm jet + Missing transverse energy final state in $p\bar{p}$ collisions at $\sqrt{s} = 1.96$ TeV

D0 Collaboration

URL <http://www-d0.fnal.gov>

(Dated: July 25, 2007)

A search for the pair production of scalar top quarks, \tilde{t} , has been performed in 995 pb^{-1} of data collected in $p\bar{p}$ collisions by the D0 detector at the Fermilab Tevatron Collider. The \tilde{t} decay mode considered is $\tilde{t} \rightarrow c\tilde{\chi}_1^0$ where $\tilde{\chi}_1^0$ is the lightest supersymmetric particle. The topology analyzed consists of two acoplanar charm jets and missing transverse energy. As a result of seeing no excess in data over the standard model prediction, sets of \tilde{t} and $\tilde{\chi}_1^0$ masses are excluded at 95% C.L. extending the domain excluded by previous searches.

Preliminary Results for Summer 2007 Conferences

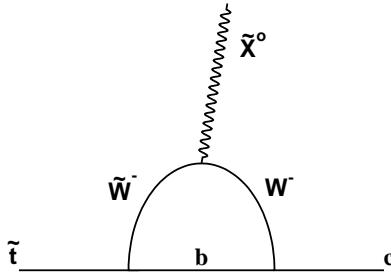


FIG. 1: Loop decay of \tilde{t} into a charm quark and neutralino.

I. INTRODUCTION

Supersymmetry (SUSY) may provide a solution to the fine tuning problem if the supersymmetric particles have masses less than 1 TeV, strongly motivating searches for SUSY objects at the Tevatron [1]. SUSY predicts the existence of partners with identical quantum numbers to all standard model (SM) particles except for a spin that differs by half a unit. There exist two spin-0 SUSY partners of the top quark, referred to as “stop” or \tilde{t} , corresponding to the top quark left and right handed states. Several arguments exist in favor of the light scalar top quark (*stop* or \tilde{t}). The large top Yukawa coupling contributes negatively when renormalization group equations are used to run the mass of stop from unification scale to the electroweak scale. In addition to that the off diagonal terms in the stop mass-squared matrix can be small due to large mixing between the superpartners of the left and right handed top quarks. This drives one of the two \tilde{t} masses to a lighter mass than all other SUSY quarks (*squarks*). Another theoretical motivation for a light stop is that if it strongly couples to the Higgs boson, it could generate a large enough CP-violating phase to provide a mechanism for electroweak baryogenesis [2].

The region of stop mass of interest considered here is $m_c + m_{\tilde{\chi}_1^0} < m_{\tilde{t}} < m_W + m_b + m_{\tilde{\chi}_1^0}$, where m_b is the b -quark mass and $\tilde{\chi}_1^0$ is the lightest of the SUSY neutralino partners of the SM neutral gauge and Higgs bosons. The search reported here assumes that $\tilde{\chi}_1^0$ is the lightest supersymmetric particle and R -Parity conservation which makes $\tilde{\chi}_1^0$ stable. The dominant stop decay mode in this model is the flavor changing process $\tilde{t} \rightarrow c\tilde{\chi}_1^0$, which proceeds via loop diagram shown in Fig. 1. In $p\bar{p}$ collisions stop pairs are produced via quark anti quark annihilation and gluon fusion. The event topology therefore consists of two acoplanar charm jets with missing transverse energy from the weakly interacting neutralinos that escape detection. At the Tevatron energy, using CTEQ6.1M parton distribution functions (PDFs) and equal renormalization and factorization scales $\mu_{rf} = m_{\tilde{t}}$, the next-to-leading-order stop pair production cross section calculated from PROSPINO [3] ranges from 15 to 1 pb for stop masses between 100 and 160 GeV, respectively, with a theoretical uncertainty of $\approx 20\%$ due to scale and PDF choices. Stop searches in the jets plus missing transverse energy mode have been reported by LEP [4], CDF [5] and D0 [6, 7]. The highest excluded stop mass to date is $m_{\tilde{t}} > 141$ GeV (95% CL) for $m_{\tilde{\chi}_1^0} = 55$ GeV [7].

II. D0 DETECTOR

A detailed description of the D0 detector can be found in [8]. The central tracking system consists of a silicon microstrip tracker and a fiber tracker, both located within a 2 T superconducting solenoidal magnet. A liquid-argon and uranium calorimeter covers pseudorapidity $|\eta|$ up to ≈ 4.2 , where $\eta = -\ln[\tan(\theta/2)]$ and θ is the polar angle with respect to the proton beam direction. An outer muon system, covering $|\eta| < 2$, consists of layers of tracking detectors and scintillation counters on both sides of 1.8 T iron toroids.

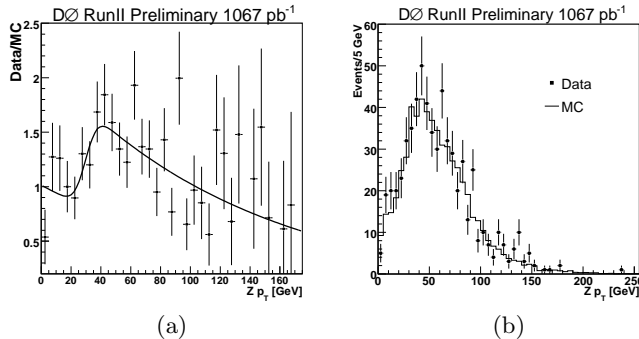


FIG. 2: (a) Ratio of the Z boson p_T spectrum superimposed with fit function. (b) Z boson p_T after applying the reweighting function to MC.

III. SIMULATED SAMPLES

Monte Carlo simulations augmented with measurements from independent D0 data samples are used for calculations of signal acceptance and efficiency, and of SM backgrounds. The largest expected backgrounds for this search are from vector bosons produced in association with jets. These processes were simulated using ALPGEN [9] interfaced with PYTHIA [10] for the generation of initial and final state radiation and hadronization. Signal samples were simulated using PYTHIA for stop masses ranging from 95 to 165 GeV and $\tilde{\chi}_1^0$ masses from 45 to 90 GeV. The PDF set CTEQ6L1 [11] was used for both signal and background samples, and all simulated events were subjected to full GEANT-based [12] simulation of the detector geometry and response. Simulated signal and background events were overlaid with randomly triggered events from data to incorporate effect of multiple interactions. After reconstruction simulated events were corrected for the differences in the luminosity profiles of the data and overlaid samples used at the generation level. The QCD multi-jet background not included in simulated samples was directly estimated from data.

IV. $Z(ee) + \text{JETS}$ STUDY

A large data sample of $Z \rightarrow ee + \text{jets}$ events from the same data period was used to improve the prediction of $Z \rightarrow \nu\bar{\nu} + \text{jets}$ and other SM backgrounds. For this study, Z boson candidates were selected using two high transverse energy ($E_T > 15$ GeV) electromagnetic clusters that deposit more than 90% of their energy in the electromagnetic calorimeter, that have shower shapes consistent with expectations for electrons, that are matched with tracks reconstructed in the central tracker, and that form an invariant mass consistent with the Z mass between 65 and 115 GeV. At this point 83,722 events were selected in a dataset corresponding to 1067 pb⁻¹ of luminosity [13]. Furthermore, at least two jets with $p_T > 15$ GeV were required where jets were reconstructed with the iterative midpoint cone algorithm with a cone size of 0.5 [14]. Additionally, the leading and second leading jets (ordered according to their transverse energies) were required to have E_T exceeding 40 and 20 GeV, respectively, and to have at least 85% of the jets' charged particle transverse momenta be associated with tracks originating from the best reconstructed primary vertex in the event. This latter track confirmation requirement on the jets removes events with spurious jets that could create anomalously large missing transverse energy.

After the jet requirements, 621 events remain in the data. The predicted number of $Z + \geq 2$ jets events were calculated using ALPGEN $Z \rightarrow ee + \text{jets}$ samples after correcting for differences in electron and jet reconstruction efficiencies between data and MC, and normalizing the MC to the inclusive number of Z events in data. A study of $Z \rightarrow ee + \text{jets}$ events showed that matching the spectrum of the transverse momentum of the Z boson predicted by ALPGEN with data required use of a reweighting function. This function was determined by fitting the ratio of the transverse momentum of the Z boson in $Z \rightarrow ee + \geq 2$ jets events in data to the ALPGEN prediction and is shown in Fig. 2(a). Figure 2(b) shows the p_T spectrum of Z boson for the same events after reweighting the MC events. After reweighting, all other kinematical variables in the $Z \rightarrow ee + \text{jets}$ sample, including the distribution of the number of reconstructed jets, applicable to the stop search were well described by MC. The QCD background in $Z \rightarrow ee + \text{jets}$ events was estimated from a fit to the dielectron invariant mass distribution over a range that included a QCD-enhanced low mass sample. The ratio of the ee events produced by γ^* photon intermediaries (DY events) to $Z + \text{DY}$ events was determined from MC and used to extract the QCD contribution by fitting the dielectron invariant mass in data with an exponential function for the QCD+DY contribution and a Breit-Wigner convolved with a Gaussian

for Z events. The number of QCD events in the inclusive Z sample was determined to be $3820 \pm 115(\text{stat}) \pm 497(\text{sys})$.

V. BACKGROUND NORMALIZATION

The predicted SM backgrounds from W + jets and Z + jets sources were normalized to the inclusive QCD background-subtracted number of $Z \rightarrow ee$ events, $N_{Z(ee)}^{\text{data}}$, determined above. Smaller $t\bar{t}$, diboson and single top contributions were normalized using the measured absolute luminosity. Equation 1 provides an explicit example of the normalization procedure, in the form of the weight assigned to a simulated $Z \rightarrow \nu\bar{\nu} + n$ light parton jets events. Similar SM weights are computed for all background processes.

$$w_{MC}^{Z(\nu\bar{\nu})+n} = f f' f'' \frac{N_{Z(ee)}^{\text{data}}}{N_{Z(\nu\bar{\nu})+n}^{MC}} \frac{\sigma_{Z(\nu\bar{\nu})+n}^{ALP}}{\sum_{k \geq 0} \sigma_{Z(ee)+k}^{ALP}} \frac{\epsilon_{Z(\nu\bar{\nu})+n}}{\epsilon_{Z(ee)+X}}. \quad (1)$$

Here, $N_{Z(\nu\bar{\nu})+n}^{MC}$ is the number of simulated $Z \rightarrow \nu\bar{\nu} + n$ light parton jets events; $\sigma_{Z(\nu\bar{\nu})+n}^{ALP}$ and $\sigma_{Z(ee)+k}^{ALP}$ are the cross sections predicted by ALPGEN for $Z \rightarrow \nu\bar{\nu} + n$ and $Z \rightarrow ee + k$ light parton jets, respectively; $\epsilon_{Z(\nu\bar{\nu})+n}$ and $\epsilon_{Z(ee)+X}$ are the corresponding detection efficiencies; $f = 0.98178 \pm 0.00068$ accommodates the fact that there is no DY contribution to $Z(\nu\bar{\nu})$ + jets events; $f' = 0.97 \pm 0.02$ accounts for the correction due to normalization of light jets to a sample that has all flavors of jets; and $f'' = 0.93 \pm 0.01$ corrects for the differences in the luminosities of stop search and $Z \rightarrow ee$ data sets. The motivation behind using this technique is to replace the cross section \times luminosity uncertainty (which is $\approx 6.1\% \oplus 15\%$ for an absolute prediction) on the predicted number of events by the 4% statistical uncertainty of the $Z \rightarrow ee + \geq 2$ jets events.

VI. DATA SAMPLE AND TRIGGER

The stop search begins with a pre-selected sample of 52M events collected from April 2003 to February 2006 with D0 three-level jets + \cancel{E}_T triggers, corresponding to an integrated luminosity of 995 pb^{-1} . The first level of trigger requires events to have either at least three calorimeter trigger towers with $E_T > 5 \text{ GeV}$, or with $E_T > 4 \text{ GeV}$ if $|\eta| > 2.6$. At the second level, \cancel{H}_T must exceed 20 GeV, where \cancel{H}_T is the missing transverse energy computed only from reconstructed jets; and the two leading jets must have an angular separation less than 168.75° . At the third level, \cancel{H}_T must exceed 30 GeV, and its angular separation from any jet must be between 25° and 180° . A parametrization of the trigger efficiency measured from the data was applied to MC events in order to fold in the trigger effects.

VII. SELECTION CRITERIA

The data sample was reduced to a final sample of 2288 potential \tilde{t} candidates, prior to application of heavy flavor tagging, by applying the 15 selection criteria denoted **C1** – **C15** and summarized in Table I.

The main motivation for **C1** was to reduce multijet backgrounds. The effect of this jet multiplicity requirement was studied using the $Z \rightarrow ee$ + jets events described earlier. The spectrum of transverse momentum of the third jet in data events with three or more jets was observed to be very well described by simulation. The $\approx 1\%$ statistical uncertainty of the bin below 20 GeV was taken as a systematic uncertainty introduced by the jet multiplicity requirement. To study the effect of the same requirement on the stop signal, where a third jet enters an event primarily through initial or final state QCD radiation, the p_T spectrum of the leading jet in simulated $Z \rightarrow ee$ events generated with PYTHIA was examined. Comparison between data and simulation showed a slight deficit in data for $p_T < 20 \text{ GeV}$; this discrepancy was used to estimate a systematic uncertainty of $\pm 1.3\%$ on the signal acceptance attributable to the jet multiplicity requirement.

Requirements **C2** to **C7** help in reducing the W + jets and multijet background; **C9** – **C11** were applied to reject W + jets background where isolated leptons arise from W decay. For an electron to be isolated the energy deposited in the calorimeter in a cone of radius 0.4 in η, ϕ space around electron direction cannot be more than 15% of the energy deposited in electromagnetic layers inside a cone of radius 0.2. A muon is declared isolated if the sum of the energies of all charged tracks other than muon in a cone of radius 0.5 around the muon direction is less than 2.5 GeV and the energy deposited in a hollow cone with inner and outer radii 0.1 and 0.4, respectively, was less than 5 GeV. A track with $p_T > 5 \text{ GeV}$ was considered isolated if no other track with $p_T > 1.5 \text{ GeV}$ was found in a hollow cone of radii 0.1 and 0.4. This condition also helps suppress backgrounds with τ leptons where the τ decays hadronically. The remaining instrumental background was removed using a quantity defined by the angular separation between any

TABLE I: Number of data events and the signal efficiencies for $m_{\tilde{t}} = 160$ and $m_{\tilde{\chi}_1^0} = 80$ GeV after each requirement.

Requirements applied	Events left	Signal eff.(%)
Events at the beginning	1426890	58.6
C1: exactly two jets	464477	32.2
C2: $\cancel{H}_T > 40$ GeV	440161	30.5
C3: $\Delta\phi(\text{jet1, jet2}) < 165^\circ$	278505	29.2
C4: jet-1 $p_T > 40$ GeV	216382	28.0
C5: jet-1 $ \eta_{det} < 1.5$	113591	27.4
C6: jet-2 $p_T > 20$ GeV	80987	24.2
C7: jet-2 $ \eta_{det} < 1.5$	62910	22.3
C8: jet-1 jet-2 CPF > 0.85	49140	22.1
C9: isolated track veto	23832	15.1
C10: isolated electron veto	23194	15.1
C11: isolated muon veto	23081	15.0
C12: $\Delta\phi_{max} - \Delta\phi_{min} < 120^\circ$	9753	14.3
C13: $A > -0.05$	3733	13.6
C14: $\Delta\phi(\text{jet}, \cancel{E}_T) > 50^\circ$	3375	13.2
C15: $\cancel{E}_T > 60$ GeV	2288	11.3

jet and the \cancel{E}_T of the event, $D = \Delta\phi_{max} - \Delta\phi_{min}$, where $\Delta\phi_{max}$ ($\Delta\phi_{min}$) is the largest(smallest) azimuthal separation between a jet and \cancel{E}_T ; and an asymmetry variable defined as $A = (\cancel{E}_T - \cancel{H}_T) / (\cancel{E}_T + \cancel{H}_T)$. Figure 3 shows that both of these variables are very powerful in eliminating multijet background.

The 2288 events selected in data can be compared to the $2018 \pm 21.45_{-285}^{+284}$ predicted from the simulation normalized to $Z \rightarrow ee$ events and $2102 \pm 22_{-364}^{+361}$ predicted using absolute luminosity normalization, with the first quoted uncertainty due to finite Monte Carlo statistics and second due to systematic effects described in more detail later. The small remaining QCD background was estimated after applying all analysis conditions except that on \cancel{E}_T , and using exponential and power law functions to extrapolate from the control region $40 \leq \cancel{E}_T \leq 60$ GeV into the signal region after subtracting SM vector boson+jets backgrounds.

VIII. HEAVY FLAVOR TAGGING AND OPTIMIZATION

After selecting the good candidate events on the basis of topology, heavy flavor tagging was used to identify charm jets in final state. A neural network (NN) tagging tool, which combines the information from three different D0 heavy flavor taggers to maximize the heavy flavor tagging efficiency, was used for this purpose. The first tagger combines the information from the impact parameter of the tracks identified in a jet into a probability that all tracks originate from primary vertex where the impact parameter of a track is its distance of closest approach to the interaction point in a plane perpendicular to the beam axis. This probability peaks towards zero for heavy flavor jets and has uniform distribution for light jets. The second tagger identifies the presence of vertices that are significantly displaced from primary vertex and associated with a jet. The third algorithm makes use of the tracks with large impact parameter significance, where the significance is defined as the ratio of the impact parameter to the uncertainty on impact parameter. The result of the combination was a NN probability which in this analysis was required to be greater than 0.2. This relatively loose requirement was necessary to keep the efficiency for detection of charm high. A trade-off is that the probability for a light parton jet to be tagged in the central part of the calorimeter for the selected operating point is $\approx 6\%$.

At the final stage of the analysis, additional selection criteria were applied which included the optimization of three kinematical variables, H_T , with H_T defined as the scalar sum of the p_T of all jets, \cancel{E}_T , and $P = \Delta\phi_{max} + \Delta\phi_{min}$. Minimum values of H_T were varied from 60 GeV to 140 GeV in steps of 20 GeV, while those for \cancel{E}_T were varied from 60 GeV to 100 GeV in steps of 10 GeV, and events having the values of these quantities above the minima were kept. Maximum values of P were tested between 240° and 320° in steps of 20° , and events having P below the maximum were retained.

For each set of requirements, the expected value of the signal confidence level (CL_s) [16] under the hypothesis that only background was present was evaluated using all stop and neutralino mass combinations, taking into account systematic uncertainties. The set of criteria that returned 5% (CL_s) for the highest neutralino mass corresponding to a given stop mass was adopted. In this procedure the lower value of theoretical stop pair production cross section was used; this was determined by subtracting the theoretical uncertainties from the nominal value of the stop production

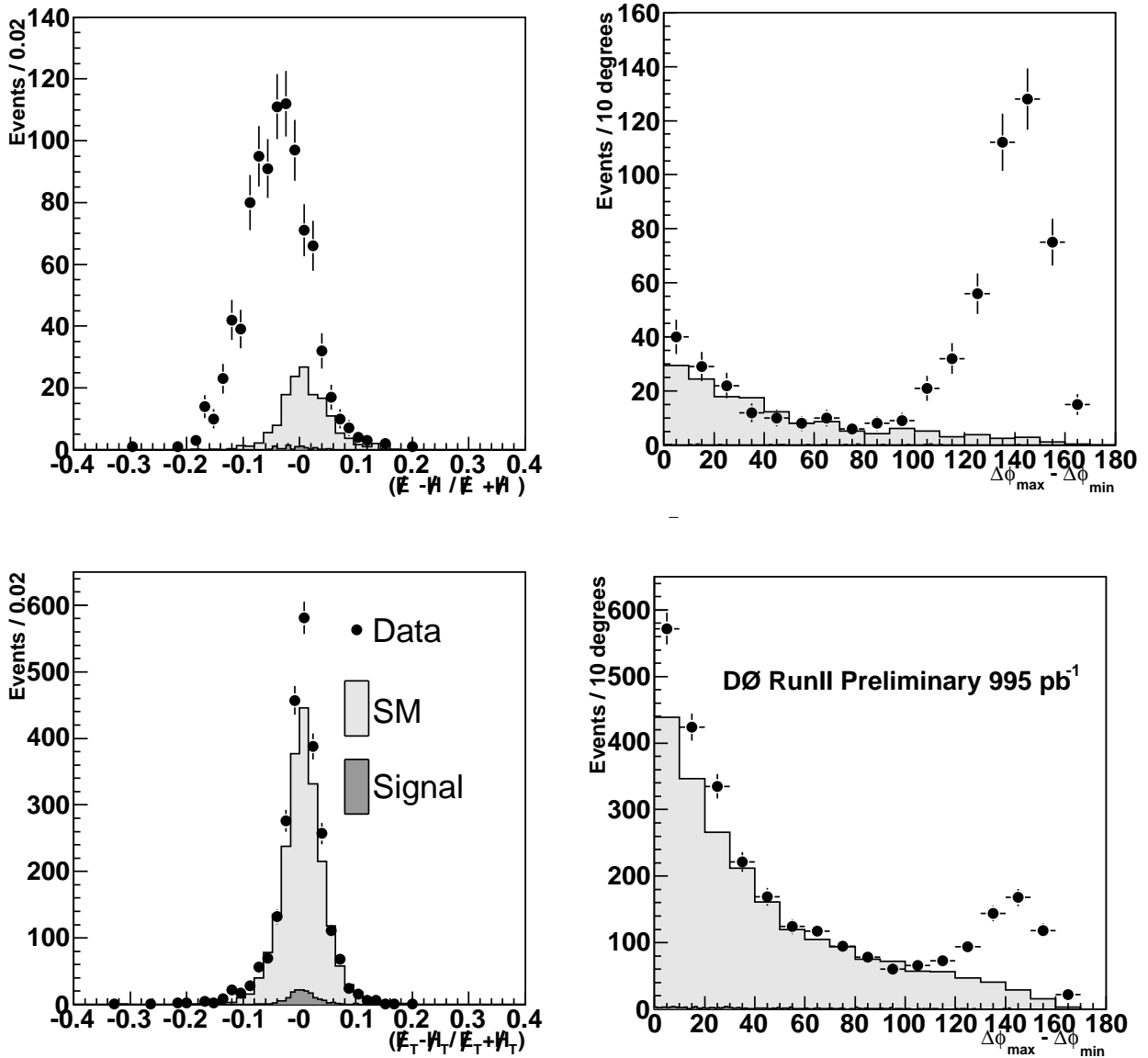


FIG. 3: Top left (Bottom left) Distribution of the asymmetry $A = (\cancel{E}_T - H_T) / (\cancel{E}_T + H_T)$ with requirement on $\Delta\phi_{max} - \Delta\phi_{min}$ inverted (applied) and of $\Delta\phi_{max} - \Delta\phi_{min}$ with requirement on A inverted (applied) top right (bottom right). A requirement on $\cancel{E}_T > 60$ GeV has been applied. The excess seen in data in lower plots for $A > -0.05$ and $\Delta\phi_{max} - \Delta\phi_{min} < 120^\circ$ is consistent with the prediction within the systematic uncertainties on the prediction.

cross section. The optimized values of the set of requirements for different stop and neutralino masses are given in Table II along with the number of events observed in data and expected SM background. In all cases $\cancel{E}_T \geq 70$ GeV was imposed. The efficiency for a representative signal mass point with $m_{\tilde{t}} = 160$ GeV and $m_{\chi_1^0} = 80$ GeV was $(2.64 \pm 0.16)\%$, with predicted number of events 26.8 ± 1.63 .

IX. SYSTEMATIC UNCERTAINTIES

Systematic uncertainties were evaluated for each stop and neutralino mass combination for the optimized set of requirements. Sources of systematic uncertainties include jet energy scale, jet resolution and identification, the

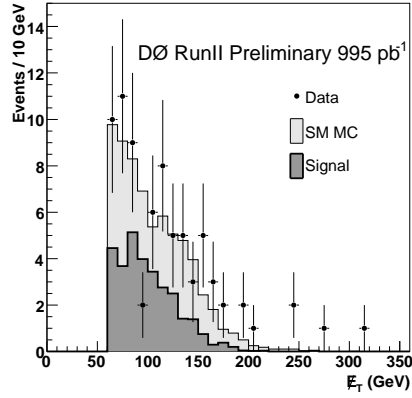


FIG. 4: Distribution of \cancel{E}_T after applying optimized requirements on H_T and P for data (points with error bars), for SM background (light filled histogram) for a signal with $m_{\tilde{t}} = 160$ GeV and $m_{\tilde{\chi}_1^0} = 80$ GeV.

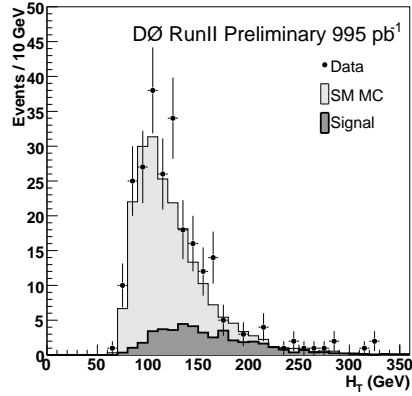


FIG. 5: Distribution of H_T after applying optimized requirements on \cancel{E}_T and P for data (points with error bars), for SM background (light filled histogram) for a signal with $m_{\tilde{t}} = 160$ GeV and $m_{\tilde{\chi}_1^0} = 80$ GeV.

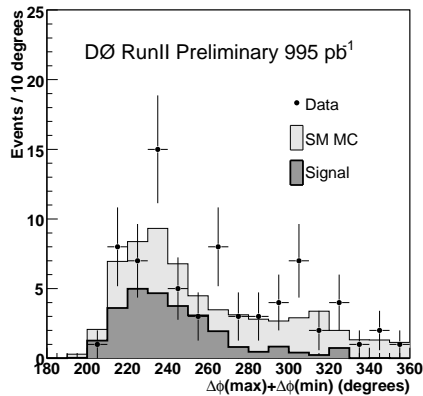


FIG. 6: Distribution of P after applying optimized requirements on \cancel{E}_T and H_T for data (points with error bars), for SM background (light filled histogram) for a signal with $m_{\tilde{t}} = 160$ GeV and $m_{\tilde{\chi}_1^0} = 80$ GeV.

$m_{\tilde{t}}$	H_T	P	# observed	#Expected
95 – 130	> 100	< 260	83	$81.9 \pm 4.0^{+13.9}_{-14.1}$
135 – 145	> 140	< 300	57	$57.1 \pm 3.1^{+8.6}_{-8.6}$
150 – 160	> 140	< 320	66	$64.2 \pm 3.2^{+9.0}_{-9.1}$

TABLE II: Optimized values of requirements, number of expected background events and observed data events. A requirement at $E_T > 70$ GeV was chosen in all cases. The values of H_T are in GeV while those for P are in degrees.

Source	SM Background	Signal
JES	+3.3%	+2%
	-5.0%	-7.6%
Jet Reso	+3%	+5%
	-1.2%	-6%
Jet ID*Reco	$\pm 0.8\%$	$\pm 0.1\%$
Trigger	$\pm 6\%$	$\pm 6\%$
Scale Factor	$\pm 5\%$	$\pm 5\%$
Normalization	$\pm 10\%$	-
Luminosity	-	6%
Taggability	$\pm 1\%$	$\pm 1\%$
Tag rate function	$\pm 4\%$	$\pm 3.3\%$
PDF choice	-	+8.7%
	-	-5.5%

TABLE III: Breakdown of systematic uncertainties on standard model background and for a signal point with $m_{\tilde{t}} = 135$ GeV and $m_{\tilde{\chi}_1^0} = 75$ GeV.

jet multiplicity requirement, trigger efficiency, data to MC scale factors, normalization of background, luminosity determination and error on the signal efficiency due to choice of PDF. These are given in Table III.

Figures 4-6 show marginal distributions for three optimized variables E_T , H_T , P with the requirement values optimized for stop masses from 150 GeV to 160 GeV.

X. RESULTS

Using the assumption that stop decays into a charm quark and neutralino with 100% branching ratio and nominal stop pair production cross section, the largest stop mass excluded by this analysis is 158 GeV for a neutralino mass of 73 GeV. With the theoretical uncertainty on the production cross section taken into account the largest excluded stop mass is 149 GeV for a neutralino mass of 63 GeV.

In summary, D0 has searched for the supersymmetric scalar partner of the top quark in the charm+neutralino final state using a sample of approximately 1 fb^{-1} . No evidence for \tilde{t} production is found, and existing constraints on \tilde{t} and $\tilde{\chi}_1^0$ are tightened. For $m_{\tilde{\chi}_1^0} = 63$ GeV, we exclude $m_{\tilde{t}} < 149$ GeV at 95% CL.

We thank the staffs at Fermilab and collaborating institutions, and acknowledge support from the DOE and NSF (USA); CEA and CNRS/IN2P3 (France); FASI, Rosatom and RFBR (Russia); CAPES, CNPq, FAPERJ, FAPESP and FUNDUNESP (Brazil); DAE and DST (India); Colciencias (Colombia); CONACyT (Mexico); KRF and KOSEF (Korea); CONICET and UBACyT (Argentina); FOM (The Netherlands); Science and Technology Facilities Council (United Kingdom); MSMT and GACR (Czech Republic); CRC Program, CFI, NSERC and WestGrid Project (Canada); BMBF and DFG (Germany); SFI (Ireland); The Swedish Research Council (Sweden); CAS and CNSF

SM process	Number of events
$W \rightarrow l\nu + \text{jets}$	20.6 ± 2.3
$Z \rightarrow \nu\nu + \text{jets}$	13.2 ± 1.8
$W \rightarrow l\nu + \text{HF} (b\bar{b}, c\bar{c})$	11.9 ± 1.1
$Z \rightarrow \nu\nu + \text{HF} (b\bar{b}, c\bar{c})$	11.6 ± 0.8
WW, WZ, ZZ	2.7 ± 0.3
$t\bar{t}$	2.3 ± 0.1
Single top	1.8 ± 0.1
$Z \rightarrow ll(e, \mu, \tau) + \text{jets}$	0.1 ± 0.1
$Z \rightarrow ll(e, \mu, \tau) + \text{HF} (b\bar{b}, c\bar{c})$	0.1 ± 0.1
Total BKG	64.3 ± 3.2
Data	66

TABLE IV: Number of expected background events from different SM sources and observed events in data for selection optimization for $m_{\tilde{t}} \geq 150$ GeV.

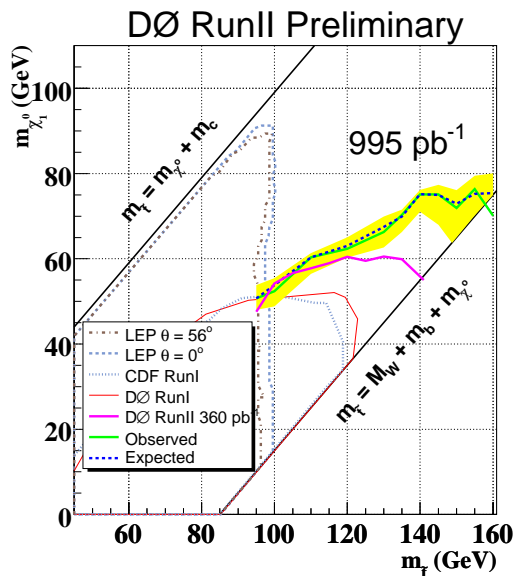


FIG. 7: Stop-neutralino mass plane excluded at 95% confidence level by present search. The observed (expected) exclusion contour is shown as the green (blue) solid (dashed) line. The yellow band represents the theoretical uncertainties on the production cross section due to PDF and renormalization and factorization scale. Results from previous searches [4–7] are also shown.

(China); Alexander von Humboldt Foundation; and the Marie Curie Program.

-
- [1] H. Baer, *et al.* Phys. Rev. D **50** 4517 (1994) and references therein.
 - [2] D. Delepine, *et al.*, Phys. Lett. B **386** 183 (1996).
 - [3] W. Beenakker, *et al.*, Nucl. Phys. B **515** 3 (1998).
 - [4] LEPSUSYWG Collaboration, ALEPH Collaboration, DELPHI collaboration, L3 Collaboration, OPAL collaboration, note LEPSUSYWG/0402.1, <http://lepsusy.web.cern.ch/lepsusy/Welcome.html>.
 - [5] T. Affolder *et al.* CDF Collaboration, Phys. Rev. Lett. **84** 5704 (2000).
 - [6] V.M. Abazov *et al.* D0 Collaboration, Phys. Rev. Lett. **93** 011801 (2004).
 - [7] V.M. Abazov *et al.* D0 Collaboration, Phys. Lett. B **645** 119 (2007).
 - [8] V.M. Abazov *et al.* (D0 Collaboration), “The upgraded DØdetector,” Nucl. Instrum. Methods **565** 463 (2006).
 - [9] M.L. Mangano, *et al.*, JHEP **0307** 001 (2003).

- [10] T. Sjöstrand *et al.*, *Comput. Phys. Commun.* **135** 238 (2001).
- [11] J. Pumplin *et al.*, *JHEP* **0207** 012 (2002) and D. Stump *et al.*, *JHEP* **0310** 046 (2003).
- [12] R. Brun and F. Carminati, CERN Program Library Long Writeup W5013, 1993 (unpublished).
- [13] T. Andeen *et. al.*, FERMILAB-TM-2365-E (2006).
- [14] G.C. Blazey *et al.*, in *Proceedings of the Workshop: QCD and Weak Boson Physics in Run II*, edited by U. Baur, R.K. Ellis, and D. Zeppenfeld, Fermilab-Pub-00/297 (2000).
- [15] W.-M. Yao *et al.*, *Journal of Physics G* **33**, 1 (2006).
- [16] T. Junk, *Nucl. Instrum. Methods A* **434** 435 (1999).